



## Mesoporous Carbon Xerogels Adsorbents for Adsorption of Cadmium and p-Nitrophenol Pollutants: Kinetic and Equilibrium Studies

Ola El-Shafey, Shaimaa El-Shafey, Nady Fathy\*



CrossMark

Surface chemistry and Catalysis Laboratory, National Research Centre, 33 El-Bohouth St., Giza, 12622 P.O., Egypt

### Abstract

Mesoporous carbon xerogels were prepared by carbonization of resorcinol-formaldehyde xerogel in presence of tannic acid as a soft-template at 700°C for 30, 60 and 90 min, respectively. Morphology, textural, surface functional surface groups and thermal analyses were measured. Their efficiency in liquid-adsorption of cadmium ions and p-nitrophenol (PNP) in a batch mode was carried out. Effect of some key factors such as pH, carbon dose, and contact time of cadmium ions and PNP as well as kinetic adsorption studies were performed. It was found that the obtained carbon xerogels of mesoporous structure have a moderate total surface area reached to 268 m<sup>2</sup>/g with various surface functional groups are effective sites for adsorbing cadmium ions and PNP from aqueous solutions. The adsorption behavior of both adsorbates on the prepared carbon samples was best described by the pseudo-second-order kinetic and Langmuir adsorption models. The maximum adsorption capacities of cadmium ions and PNP were 99 and 133 mg/g, respectively; onto the prepared carbon xerogel at 700°C and 60 min. As a result of these observations, the produced mesoporous carbon samples are very effective adsorbents for extracting considerable amounts of cadmium ions and PNP from aqueous solutions.

**Keywords:** Carbon xerogels; adsorption; cadmium ions; para-nitrophenol; equilibrium studies

### 1. Introduction

In order to enhance the performance of carbon materials as adsorbents, catalysts or catalyst supports, many researchers accommodated between the porous structure and chemical surface properties of them, which in turn, control the strength of the interactions between the surface of carbon material and the corresponding target molecule [1-5]. One of the main advantages of carbon xerogels is their versatility in both porous structure and physicochemical properties that can be easily modified to one specific application. The most common synthesis of such materials is via the polycondensation of resorcinol with formaldehyde in water as solvent and a basic or acid catalyst followed by drying in a conventional dryer and then carbonization at elevated temperatures [2, 3, 5].

For environmental tasks, activated carbons (ACs); among various adsorbents, is still by far the most important one in current use in the environmental pollution. This is mainly attributed to

its large surface area, high adsorption capacity to a limit extent, microporous structure and selective adsorption [4, 6, 7]. However, the dominance of micropores (<2 nm) in ACs limits the transport of metal ions, hydrated metal ions and large molecules through the surface of ACs into inside pores. Thus, it is essential to produce mesoporous carbon adsorbents with both accessible pores and surface active sites [8, 9] which would improve the adsorption rate and efficiency [10]. Accordingly, the remediation of several pollutants such as heavy metals and organics introduced into surface water during discharging wastewater of many industries is a target of many researchers nowadays. Increasing the accumulative dose of heavy metals (such as lead, mercury, copper, zinc and cadmium) in water which do not degrade biologically like some organics can be caused major concerns because they can affair poisoning, cancer and nervous system damages. [8, 11-15]. In particular, the accumulation of cadmium in drinking water can affair some diseases such as lung

\*Corresponding author e-mail: [na.fathy@nrc.sci.eg](mailto:na.fathy@nrc.sci.eg), [fathyna.77@hotmail.com](mailto:fathyna.77@hotmail.com)

Receive Date: 03 August 2021, Revise Date: 16 August 2021, Accept Date: 17 August 2021

DOI: 10.21608/EJCHEM.2021.89014.4274

©2022 National Information and Documentation Center (NIDOC)

insufficiency, muscular cramps, cancer, diarrhea, nausea and renal degradation [14, 15]. Many techniques have been used in the literature to reduce the dosage of these metals in water, such as chemical oxidation, reduction, precipitation, membrane filtration, ion exchange, and adsorption [8, 11-15]. Adsorption has been reported to be a promising technique for the removal of metal ions from wastewater sources due to its simplicity, economics, and appropriateness during removal operations, and it can pave the way to discover innovative and high-efficiency adsorbents.

On the other hand, organic chemicals such as phenolic derivatives are disposed very frequently in wastewater from heavy chemical, petrochemical, and oil refining industries [16-19]. Therefore, removal to less noxious structures of phenolic compounds is essential for purification of wastewaters as well as raw water. In particular, para-nitrophenol (PNP) is mostly applied as a model of phenolic contaminant [18, 19].

In this paper, carbon xerogels were prepared by carbonization of resorcinol-formaldehyde xerogel in presence of tannic acid as a soft-template at 700°C for 30, 60 and 90 min, respectively. The removal of cadmium ions and PNP over prepared mesoporous carbon xerogels was carried out. The batch mode adsorption was selected due to its simplicity. The influence of some key factors such as pH, carbon dose, and contact time of metal ions and PNP were investigated. Kinetic adsorption studies were performed using pseudo-first-order, pseudo-second-order and intraparticle diffusion models to determine the mechanism of adsorption. The adsorption isotherm studies of cadmium and PNP species were determined by a batch operation at pH of 5 and room temperature of 25°C. The equilibrium adsorption data were analyzed using Langmuir and Freundlich isotherms to specify the type of adsorption process on the surface of adsorbents.

## 2. Materials and methods

### 2.1. Materials

As carbon xerogel source, resorcinol (R, C<sub>6</sub>H<sub>4</sub>(OH)<sub>2</sub>, Panreac, 99%) was polymerized with formaldehyde (HCHO, 37%, Aldrich), methanol (CH<sub>3</sub>OH, Aldrich, 99%), and sodium carbonate (Na<sub>2</sub>CO<sub>3</sub>, Lab Rasayan, 99%) as catalyst. Tannic acid (TA, C<sub>76</sub>H<sub>52</sub>O<sub>46</sub>, SDFCL, 99%) was used as a soft template to avoid shrinkage during drying and carbonization process. Ammonia solution (NH<sub>4</sub>OH, Adwic, 25–28%) and nitric acid (HNO<sub>3</sub>, Alpha Chemika, 60–63%) were applied for adjusting pH. Acetone (CH<sub>3</sub>COCH<sub>3</sub>, Adwic, 96%) was used for solvent exchange during the drying process.

### 2.2. Synthesis of mesoporous carbon xerogels

The preparation method includes two steps; the first is sol-gel step and second one is the carbonization of prepared gel at 700°C within different times. Typically, about 4.24 g of R and 7.99 g of TA were dissolved in a 20 ml of methanol as a solvent at 25°C, followed by slow addition of F (14.8 mL). Then, NH<sub>4</sub>OH (0.5 mmol L<sup>-1</sup>) was added into R/TA/F solution under vigorous stirring to pH 10. After that, low amount of dissolved Na<sub>2</sub>CO<sub>3</sub> in distilled H<sub>2</sub>O was added as catalyst. A dark brown homogenous sol was observed and started to form the alcogel after 20 min through raising temperature from 25 to 80°C. The formed alcogel was immersed in acetone solution for exchanging with methanol and water to avoid shrinkage during the conventional drying step. After pulling gel from acetone, the gel was dried in air-oven at 90°C for 4 h and overnight at 110°C. Then, some portions of the dried gel were carbonized at 700°C under N<sub>2</sub> gas flow for 30, 60 and 90 min. The symbols of prepared carbon xerogels were labelled as CX-700-30, CX-700-60 and CX-700-90.

### 2.3. Characterization tools

Scanning electron microscopy of JEOL JXA-840A and transmission electron microscopy (JEOL model, TEM-1230 Electron analyzer) were used to visualize the surface morphology of selected carbon xerogel. Before scanning run, the sample was coated with gold using quick auto-coaters (JFC-I500, JEOL). Thermogravimetric analysis (TGA) was performed under N<sub>2</sub> atmosphere with heating rate of 10°/min using TGAQ500V20.10 Build (universalV3.9A, TA instruments). The sample was put in silica crucible and subject to pyrolysis program starting from room temperature to 800°C. Fourier transform infrared spectroscopy (FTIR) was recorded within the wavenumber range 4000–400 cm<sup>-1</sup> using a spectrophotometer of FTIR-2000 Perkin Elmer (USA), employing pressed KBr-pellets with a mass ratio of 0.002 sample/0.998 KBr (g/g) and then scanned. Moreover, the porous properties of the prepared samples were evaluated using N<sub>2</sub> adsorption analysis at -196°C (BEL-Sorp, Microtrac Bel Crop, Japan) as listed in Table 1.

### 2.4. Adsorption experiments

The main objective of this study was to assess the feasibility of mesoporous carbon xerogels in

adsorption of Cd (II) and p-nitrophenol (PNP) from their aqueous solutions. Stock solutions of each Cd (II) and PNP with initial concentration of 500 mg/L were prepared. The effect of the following parameters on the kinetic removal of both pollutants was studied: (i) pH variable (2-8) (ii) carbon dose (0.01 – 0.1 g) and (iii) agitation time (0–180 min) at a temperature (25°C). In each batch adsorption round, about 100 mg of dried powder carbon adsorbent was added into a 100 mL of Cd (II) ions and PNP solutions, separately; with those initial concentrations in a 250mL stopper conical flasks under shaking at 150 rpm for the desired time at 25°C. Initial concentrations of Cd (II) ions and PNP pollutants with initial concentrations (20-200 mg/L) and (100-500 mg/L), respectively, were conducted to study the isotherm and mechanism of adsorption. At the end of the adsorption period, the solution sample (2ml) was taken and filtered using filter paper of Whatman No.45. The residual concentrations of Cd (II) ions in aqueous solutions were measured by atomic absorption spectrophotometer (AAS, a Perkin –Elmer model 2380) at wavelength equal 485nm. For determination PNP residual concentration, its absorbance value was taken at wavelength of 317 nm by using a UV–Vis spectrophotometer (Shimadzu-2401PC).

### 2.5. Kinetic and equilibrium studies

The amount of adsorbate adsorbed onto the prepared adsorbents at equilibrium ( $q_e$ , mg/g) or at time  $t$  ( $q_t$ , mg/g) was calculated according to the following equations:

$$q_e = \frac{(C_0 - C_e)V}{m} \quad (1)$$

$$q_t = \frac{(C_0 - C_t)V}{m} \quad (2)$$

where  $C_0$ ,  $C_e$ , and  $C_t$  are initial, equilibrium and time concentrations (mg/L) of adsorbate, respectively.  $V$  is the volume of solution (mL) and  $m$  is the mass of adsorbent (mg). The effect of the contact time (0-180 min) was carried out to investigate the kinetic models such as:

Lagergren-first-order kinetic model which can be described by the equation [20]:

$$\log (q_e - q_t) = \log q_e - \frac{k_1 t}{2.303} \quad (3)$$

While pseudo-second-order kinetic model which is expressed by the equation [21]:

$$\frac{t}{q_t} = \frac{1}{k_2 q_e^2} + \frac{t}{q_e} \quad (4)$$

where  $q_e$  and  $q_t$  are the adsorbed amounts of adsorbate (mg/g) at equilibrium and time  $t$  (min), respectively;  $k_1$  is the rate constant of the Lagergren-first-order kinetic model ( $\text{min}^{-1}$ ). The values of  $k_1$  were calculated from the plots of  $\log (q_e - q_t)$  versus  $t$ . In equation (4),  $k_2$  is the rate constant ( $\text{g/mg min}$ ) of pseudo-second-order kinetic model of adsorption. The slope and intercept of the linear plots  $t/q_t$  against  $t$  yield the values of  $1/q_e$  and  $1/k_2 q_e^2$ .

The intra-particle diffusion model as proposed by Weber and Morris [22] is described by the equation:

$$q_t = k_{id} t^{1/2} + C \quad (5)$$

where  $C$  (mg/g) is the intercept and  $k_{id}$  is the intra-particle diffusion rate constant ( $\text{mg/g min}^{1/2}$ ), which can be calculated from the slope of the linear plots of  $q_t$  versus  $t^{1/2}$ . All the calculated kinetic parameters are summarized in Table 2.

To examine the equilibrium adsorption of adsorbates onto the prepared adsorbents, thus the adsorption data were analyzed in terms of Langmuir and Freundlich isotherms. The linear form of the Langmuir isotherm [23] is expressed as the following equation:

$$C_e / q_e = \frac{1}{K_L Q_m} + \frac{1}{Q_m} C_e \quad (6)$$

where  $C_e$  is the equilibrium concentration of adsorbate (mg/L),  $q_e$  the amount of adsorbate adsorbed at equilibrium (mg/g), and  $Q_m$  is the monolayer adsorption capacity (mg/g) and  $K_L$  (L/mg) is the Langmuir adsorption equilibrium constant. The free energy of adsorption,  $\Delta G$  (kJ/mol) can also be evaluated from the parameter  $K_L$  according to the expression:

$$\Delta G = -RT \ln K_L \quad (7)$$

In addition Langmuir adsorption isotherm can be given in expression of a dimensionless constant called a "separation factor" and noted as ( $R_L$ ):

$$R_L = \frac{1}{1 + K_L C_0} \quad (8)$$

The equation representing linear form of Freundlich adsorption [24] can be given as:

$$\log q_e = \log K_f + \frac{1}{n} \log C_e \quad (9)$$

where  $K_F$  ( $\text{mg/g (L/mg)}^{1/n}$ ) is roughly an indicator of the adsorption capacity and  $1/n$  is the adsorption intensity. Freundlich constants  $K_F$  and  $1/n$  can be calculated from the intercept and slope of the linear plot with  $\log q_e$  against  $\log C_e$ . To justify the applicability of each isotherm, the correlation coefficient ( $R^2$ ) was calculated.

### 3. Results and discussion

#### 3.1. Surface characteristics of adsorbents

It is essential to elucidate the morphology of adsorbent to investigate the surface properties of adsorbent. Fig. 1 (a and b) shows both SEM and TEM images of selected sample (CX-700-60). It can be deduced that the carbonization of resorcinol and formaldehyde gels in presence of tannic acid as soft template produced semi-spherical carbon particles appearing as interconnected nodules. The size of developed carbon particles is ranged between 50 and 120 nm as calculated from TEM. Otherwise, carbon xerogels formulated from only resorcinol-formaldehyde organic gels had spherical carbons with lower sizes than 50 nm; however, their porous structures companied with large shrinkage during drying and carbonization as reported in elsewhere [9, 10, 25–28]. In the TEM image (Fig. 1b) it can be seen formation of intercluster voids confirming the generation of the mesopores into CX network.

Fig. 2 displays FTIR spectra of the carbonized samples at 700°C for 30, 60 and 90 min, respectively. The surface functional groups in all samples are similar; however, a considerable reduction in their intensities is observed with increasing in the carbonization time. Moreover, the samples are enriched in oxygen functional groups such as  $-\text{OH}$ ,  $\text{COO}^-$ ,  $\text{C}=\text{O}$  and  $\text{C}-\text{O}$  [3, 9, 10]. For example, the boarder band at  $3420\text{ cm}^{-1}$  is associated to H-bonded water molecules, to hydroxyl groups from carbonyls, phenols or alcohols. A shoulder band at  $1712\text{ cm}^{-1}$  is assigned to  $\text{C}=\text{O}$  stretching vibration in ketenes, aldehydes, lactones or carboxylic groups which disappeared in CX-700-90. At  $1620\text{ cm}^{-1}$ , sharper band is assigned to  $\text{C}=\text{C}$  aromatic skeletal stretching or conjugated  $\text{C}=\text{O}$  stretching vibration in aromatic system [3, 9, 10]. Bands between  $1300$  and  $900\text{ cm}^{-1}$  in all spectra are currently assigned to  $\text{C}-\text{O}$  stretching in acids, alcohols, phenols, ethers, and esters.

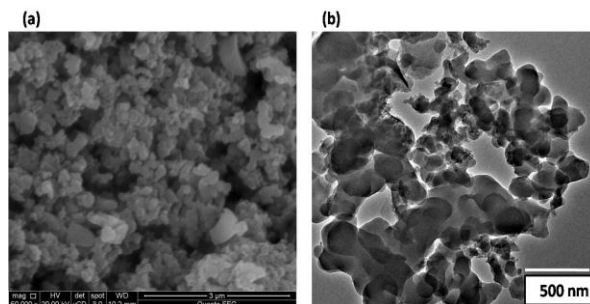


Fig. 1: (a) SEM and (b) TEM images of CX-700-60 adsorbent.

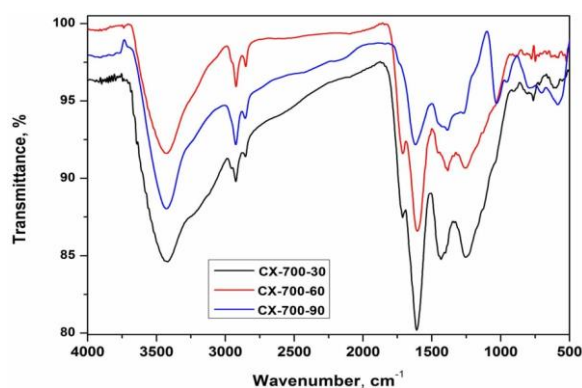


Fig. 2: FTIR spectra of the investigated samples.

In order to follow the changes in the thermal behavior of prepared carbon xerogels, CX-700-60 was selected as shown in Fig. 3. This sample was subjected to the thermo-analytical measurements up to  $800^\circ\text{C}$  under flowing  $\text{N}_2$  gas. The dramatic thermal decomposition in TGA of CX-700-60 is occurred after  $350^\circ\text{C}$  (88% weight is fixed) till  $800^\circ\text{C}$  (17% weight is fixed). About 6% of sample is decomposed till  $100^\circ\text{C}$  due to the release of water and solvents, followed by further 6% of weight loss is happened up to  $350^\circ\text{C}$  which is resulted from decomposition of light organics to  $\text{CO}_2$  and  $\text{CH}_4$  gases. After this temperature, larger organics in carbon network are decomposed gradually with formation  $\text{CO}$  gases at higher temperatures confirming that gasification process of carbon sample is high [3]. This could be ascribed to the high O-content of the surface which enhances the self gasification reaction [3, 28]. From these findings, the prepared samples exhibited superb thermal stability.

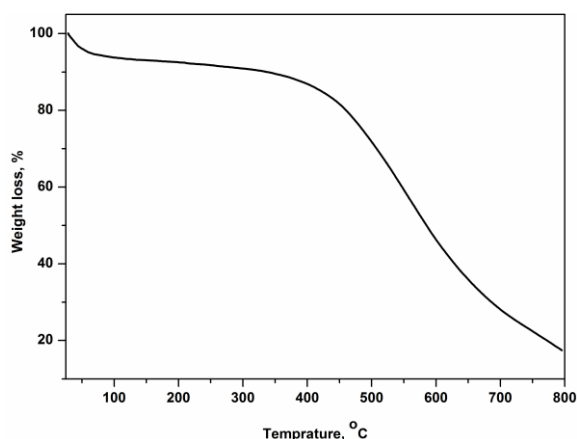


Fig. 3: TGA profile of the prepared CX-700-60 sample.

### 3.2. Textural properties of samples

Evaluation of the microporosity and mesoporosity development in the prepared samples was employed with regarding to the following parameters: the BET surface area ( $S_{BET}$ ,  $m^2/g$ ), total pore volume at relative pressure  $P/P_0 = 0.97$  ( $V_P$ ,  $cm^3/g$ ), mean pore radius ( $W_P$ ,  $\text{Å}$ ) was calculated from  $(2V_P/S_{BET}) \times 10^4$ , micropore volume ( $V_{micro}$ ,  $cm^3/g$ ) and micropore surface area ( $S_{micro}$ ,  $m^2/g$ ) were calculated from the t-plot theory and mesopore volume ( $V_{meso}$ ,  $cm^3/g$ ) from the difference between  $V_P$  and  $V_{micro}$  as listed in Table 1.

When the organic gel exposed to thermal carbonization at  $700^\circ\text{C}$  during different times, it was found that increasing time from 30 to 60 min developed well-porosity with high total surface area in CX-700-60. Whereas the higher time of carbonization could be inhibited the total porosity as shown in CX-700-90. Also, CX-700-60 sample has high total surface area and mesoporosity reached to 64.7% which could enhance the adsorption of heavy metals and organics from aqueous solution. Therefore, good quality adsorbent carbons can be obtained by heat treatment at  $700^\circ\text{C}$  for 60 min. Overall, mesoporous carbon xerogels are synthesized successfully using tannic acid as template through sol-gel process of resorcinol with formaldehyde followed by drying and then pyrolysis at  $700^\circ\text{C}$  with different times.

### 3.3. Adsorption studies of cadmium (II) ions by the samples

In order to find the suitable pH working and carbon dose in removal of cadmium ions by the prepared carbons. Cadmium solutions ( $C_0 = 50$  mg/L) with different pH values (2, 4, 5, 7 and 8) were performed with 0.04 g of each sample as shown in Fig. 4a. The maximum Cd(II) removal occurred in the pH range 5–8 while removal of cadmium was very slightly at pH 2 [14, 29, 30]. At pH 8, the

removal of cadmium was completely occurred onto CX-700-60. It has been reported that at pH 8.0, the species distribution is approximately 90%  $\text{Cd}^{2+}$  and 10%  $\text{Cd}(\text{OH})^+$  [30]. The maximum removal was occurred at pH of 5.

Table 1: Porosity parameters developed in the investigated carbon xerogels.

Sample notation	$S_{BET}$ ( $m^2/g$ )	$V_P$ ( $cm^3/g$ )	$W_P$ ( $\text{Å}$ )	$S_{micro}$ (t-plot) ( $m^2/g$ )	$V_{micro}$ (t-plot) ( $cm^3/g$ )	$V_{meso}$ ( $cm^3/g$ )	% $V_{meso}$
CX-700-30	136	0.114	16.8	70	0.042	0.072	63.2
CX700-60	268	0.244	18.2	141	0.086	0.158	64.7
CX700-90	225	0.188	16.7	115	0.074	0.114	60.6

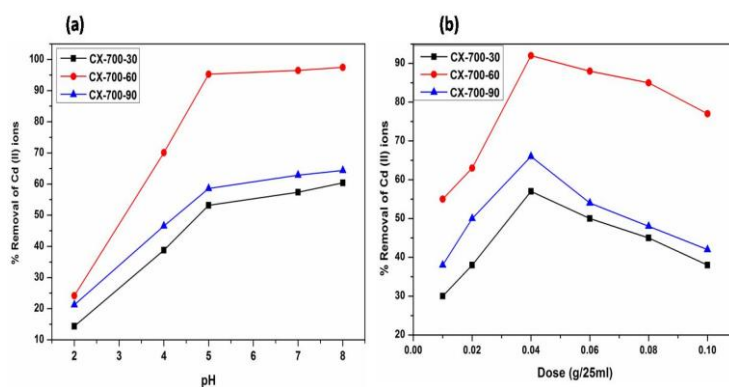
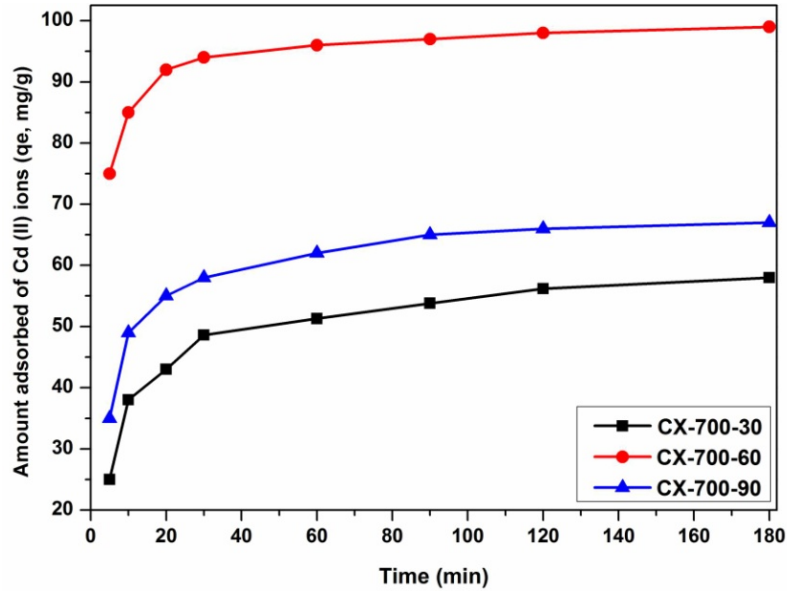


Fig. 4: Effects of (a) pH variable ( $C_0 = 50$  mg/L,  $m = 0.04$  g,  $V = 25$  ml, time = 2 h and  $T = 25^\circ\text{C}$ ) and (b) carbon dose on the removal of Cd (II) ions from aqueous solutions ( $C_0 = 50$  mg/L,  $V = 25$  ml, time = 2 h and  $T = 25^\circ\text{C}$ ).

Carbon dose effect within different values (0.01 to 0.1 g/25 mL) with initial concentration of Cd (II) ions equal to 50mg/L was tested as shown in Fig. 4b. The highest removal of Cd (II) ions was discovered at 0.04 g of all samples, after which there was reduction in removal efficiency. Accordingly, over the optimum carbon dose (0.04 g); an aggregation phenomenon is happened and led to a decrease in the available surface area followed by a decrease in adsorption efficiency [14, 29].

At initial concentration of 100 mg/L in 100 mL aqueous solution conducted with 0.1 g of sample, effect of contact time is studied as depicted in Fig. 5. Adsorption of Cd (II) is increased frequently with an increasing in the contact time. The equilibrium time is started at 30 min over the surface of tested adsorbents. The highest sample of total surface area and mesopores (CX-700-60) exhibited superior adsorption of cadmium at 5 min (75mg/g) which reached to 98 mg/g at 180 min.



**Fig. 5:** Effect of contact time on the amount adsorbed of Cd (II) ions onto carbon samples as a function of  $C_0 = 100$  mg/L,  $m = 0.1$  g,  $V = 100$  ml,  $\text{pH} = 5$  and  $T = 25^\circ\text{C}$ .

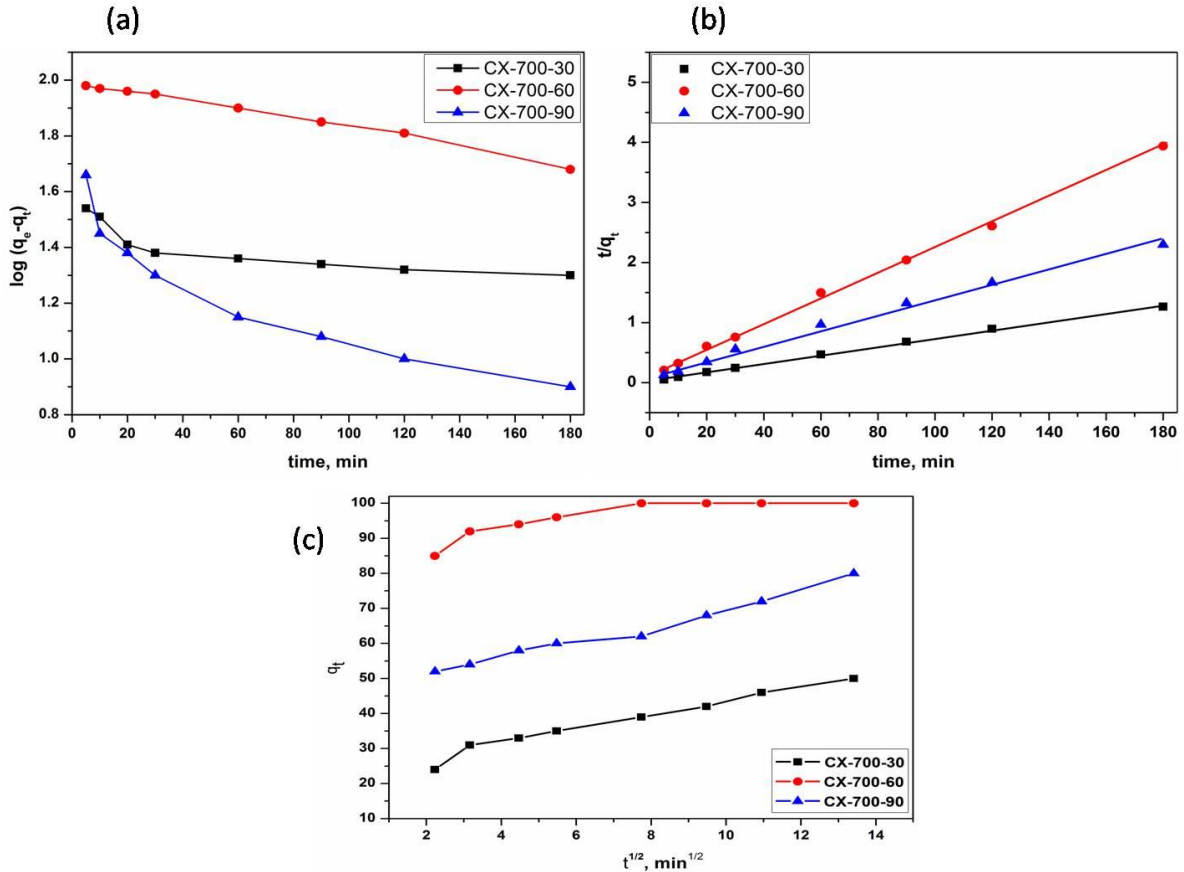


**Fig. 6:** Plots of (a) pseudo-first order kinetic (b) pseudo-second order kinetic and (c) Intraparticle diffusion models ( $C_0 = 100$  mg/L,  $m = 0.04$  g,  $V = 100$  ml,  $\text{pH} = 5$  and  $T = 25^\circ\text{C}$ ).

Kinetic studies of Cd (II) adsorption by using three kinetic models are estimated and drawn in Fig. 6. The calculated constants of those models are listed in Table 2. Correlation coefficients ( $r^2$ ) of pseudo-first order and pseudo-second order kinetic models are summarized in Table 2. The straight lines in plot of linear pseudo-second order equation showed good agreement of experimental data given higher correlation coefficients closed to unity as compared to pseudo-first order kinetic model. This affirms that the adsorption of Cd (II) onto prepared carbons is most suitably represented by a pseudo-second order rate process. Moreover, the intraparticle diffusion plots showed two stages of adsorption as seen in Fig 6c. The first linear portion refers to the boundary layer diffusion (film diffusion) and the latter portion is owing to the intraparticle diffusion [14, 29]. This result indicates that the adsorption process proceeds by surface adsorption and intraparticle diffusion.

Equilibrium adsorption is also analyzed using two-known models such as Langmuir and Freundlich isotherms. Table 3 lists the values deduced from both isotherms as well as their correlation coefficients ( $r^2$ ). The cadmium adsorption capacity ( $Q_m$ , mg/g) by the obtained carbon adsorbents was found to be in the decreasing order as follows: CX-700-60 > CX700-90 > CX-700-30. The Langmuir equation fitted the data better than the Freundlich equation by describing the data over the entire concentration range (100-500 mg/L) due to they have higher  $r^2$  values. Table 4 shows comparison adsorption capacity of different adsorbents toward adsorption of cadmium. It can be indicated that the prepared carbons exhibited superior adsorption capacity as compared to other reported carbon adsorbents such as activated carbons and carbon nanotubes. This finding may be attributed to their morphology and mesopores in their porous structure which are proper for uptaking cadmium ions.

**Table 2:** Adsorption kinetic constants for adsorption of Cd (II) ions by the investigated carbon xerogels (carbon weight = 0.1 g, volume =100 mL, pH= 5 and temperature= 25°C).

Samples	$C_0$ (mg/L)	First order kinetic			Second order kinetic				Intraparticle diffusion	
		$q_{e1}$ (mg/g)	$k_1$ ( $min^{-1}$ )	$r^2$	$q_{e2}$ (mg/g)	$k_2$ (g/mg min)	$h$ (mg/g min)	$q_{e2}$ (mg/g)	$K_{id}$ ( $mg/g min^{0.5}$ )	$q_{e1}$ (mg/g)
CX-700-30	100	28.6	0.010	0.887	28.7	$3.01 \times 10^{-4}$	0.248	0.999	1.03	15.0
CX-700-60	100	55.9	0.016	0.977	97.3	$9.03 \times 10^{-5}$	0.238	0.995	1.84	23.9
CX-700-90	100	42.2	0.002	0.940	67.1	$1.10 \times 10^{-4}$	0.495	0.996	3.28	11.3

**Table 3:** Langmuir and Freundlich constants for the adsorption of Cd (II) ions.

Sample Notation	Langmuir parameters					Freundlich parameters		
	$Q_m$ mg/g	$K_L$ L/g	$R_L$	$\Delta G^0$ kJ/mol	$r^2$	$K_F$	1/n	$r^2$
CX700-30	57	0.0345	0.168	- 18.6	0.998	3.6	0.632	0.911
CX700-60	99	0.0737	0.127	- 19.7	0.998	11.1	0.420	0.922
CX700-90	74	0.0418	0.145	- 19.3	0.999	9.5	0.449	0.915

**Table 4:** Comparison of adsorption capacities of Cd (II) ions onto different carbon adsorbents

Adsorbents	$S_{BET}$ ( $m^2/g$ )	Amount adsorbed (mg/g)	Refs
Activated carbons-common reed	1193	83.4	[14]
Activated carbon- cotton stalks	253	31.6	[29]
Activated carbons	130.4-234.4	40.9-48.1	[31]
Carbon nanotubes	60	~ 17.9	[32]
Carbon xerogels	136-268	57-99	This work

### 3.4. Adsorption studies of p-nitrophenol by the samples

Fig. 7 (a) depicts the effect of pH variation between values of 2 and 8 on the removal of PNP onto the prepared carbons with initial concentration 100mg/L, carbon dose of 0.04g and volume 25 mL at 25°C. At pH range of 2 to 5, all samples showed increase in removal percentage as pH increased from 2 to 5, and the maximum removal (37, 66 and 55 % by CX700-30, CX-700-60 and CX-700-90,

respectively) occurred at pH of 5 where molecular PNP existed in the solution.

By increasing pH to 6 and 8, the removal percentage decreased due to the electrostatic repulsions between the negatively charged surface of samples and anionic forms of PNP [33]. Thus the highest removal occurred at pH of 5 which be used in next adsorption experiments.

Fig. 7b describes the effect of carbon dose (0.01 to 0.1 g/25 mL) with 50mg/L of PNP at 25°C. As cadmium adsorption, the optimum carbon dose occurred at 0.04 g/25mL. Over this dose, the adsorption of PNP decreased because of the active sites in the samples become saturated and undergo aggregation, thereby reducing their adsorption capacities [34].

Fig. 7c illustrates the results obtained from effect of contact time on the amount adsorbed of PNP when an initial concentration of 100 mg/L in 100 mL aqueous solution conducted with 0.1 g of sample. Fast PNP adsorption is observed with increasing the

contact time and CX-700-60 showed the better adsorption than other tested samples. Table 5 lists the kinetic constants derived pseudo-first order, pseudo-second order kinetic and intraparticle diffusion models with their correlation coefficients ( $r^2$ ) to explore the possible mechanism of p-nitrophenol adsorption on the samples. Results indicate that pseudo-second order kinetic can satisfactorily fit the kinetic data based on the high  $r^2$  (0.959–0.991). This finding means that the adsorption process is controlled by chemisorption on the surface on adsorbent.

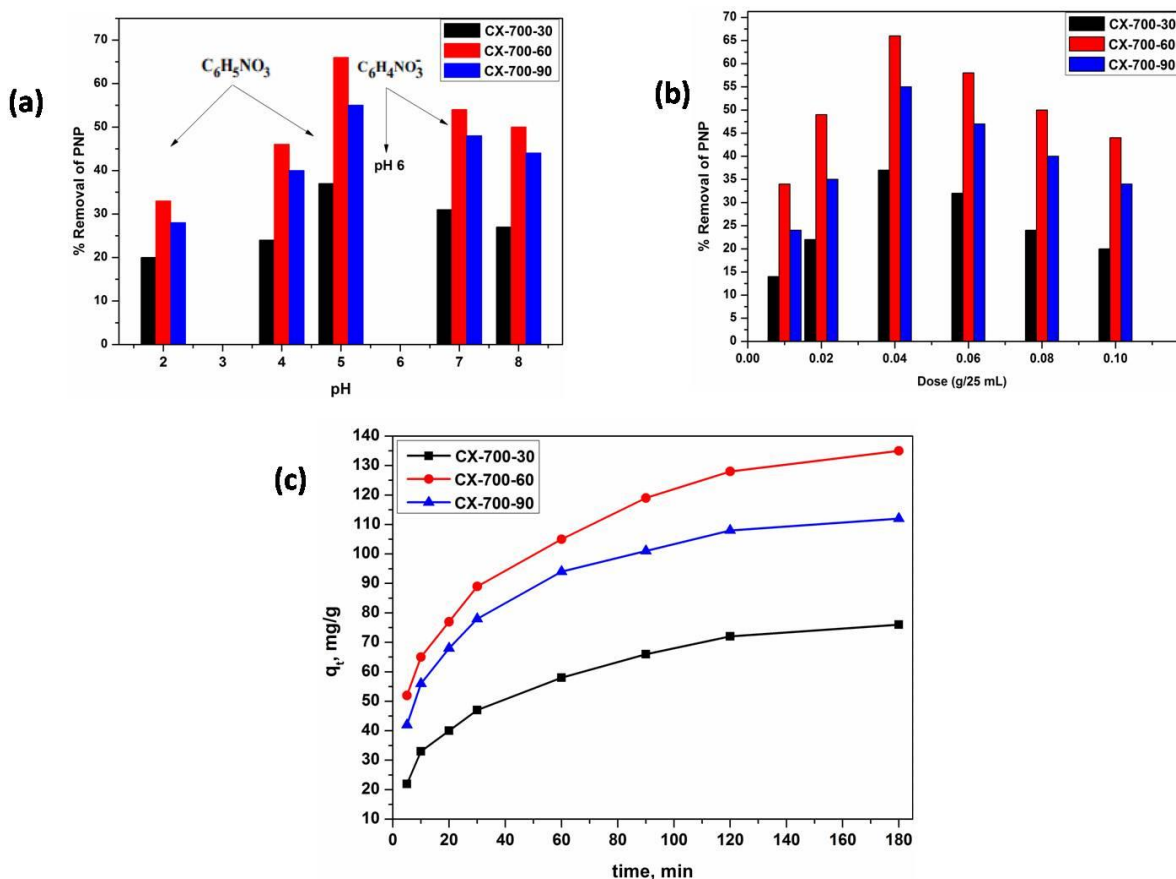


**Fig. 7:** Effects of (a) pH variable ( $C_0 = 50$  mg/L,  $m = 0.04$  g,  $V = 25$  ml, time = 2 h and  $T = 25^\circ\text{C}$ ); (b) carbon dose ( $C_0 = 50$  mg/L,  $V = 25$  ml, time = 2 h and  $T = 25^\circ\text{C}$ ) and (c) contact time on the removal of PNP from aqueous solutions ( $C_0 = 100$  mg/L,  $V = 100$  mL,  $\text{pH} = 5$  and  $T = 25^\circ\text{C}$ ).

Adsorption isotherms are provided for the adsorption of PNP on CX-700-30, CX-700-60 and CX-700-90 samples as shown in Fig. 8. The results indicated that the adsorption of PNP is described well with L-type (Langmuir) isotherm confirming that monolayer adsorption took place on the surface with a range of p-nitrophenol concentrations (100, 150, 200, 300, 400 and 500 mg/L). It was found that Langmuir isotherm displayed high values of  $r^2$  (0.997-0.999) and is a more suitable model to explain

the adsorption behavior of PNP. The maximum adsorption quantity ( $Q_m$ ) of PNP onto CX-700-30, CX-700-60 and CX-700-90 samples was found to 69, 133 and 103 mg/g, respectively. In a particular, CX-700-60 showed the highest adsorption capacity. Also, the calculated Langmuir characteristics parameter (or separation factor,  $R_L$ ) strongly indicate that the adsorption process of PNP is a favorable, where the values of  $R_L$  are much less than 1.0.



The negative value of  $\Delta G^\circ$  means that the adsorption of PNP is a spontaneous and physisorption process as a result of interaction of  $\pi$ -electron region of the aromatic structures of carbon surface with the electron acceptor on the aromatic ring of p-

nitrophenol *via*  $\pi$ - $\pi$  interactions [18, 19, 32]. In a conclusion, good adsorbing mesoporous carbons are obtained by carbonization of resorcinol-formaldehyde templated on tannic acid, as observed by the uptake of p-nitrophenol from aqueous solutions.

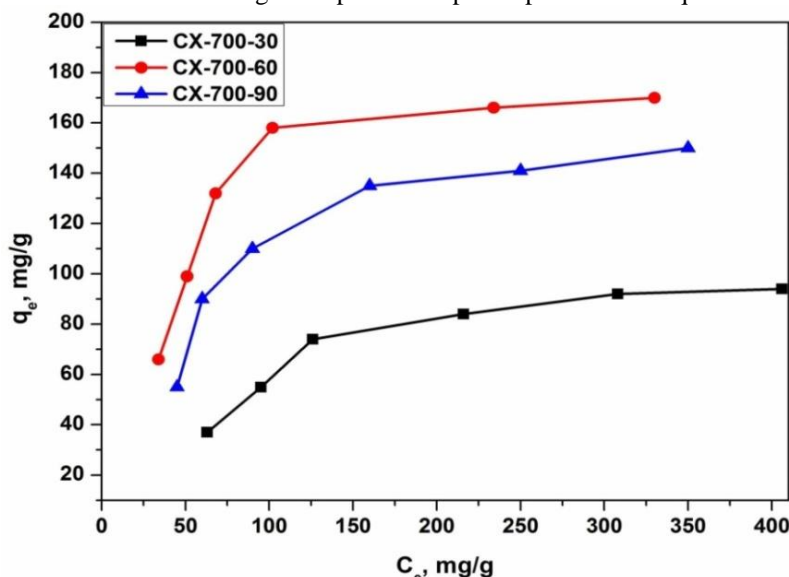


Fig. 8: Adsorption isotherms of PNP onto the prepared samples (pH= 5 and T = 25°C)

Table 6: Langmuir and Freundlich constants for the adsorption of PNP.

Sample Notation	Langmuir parameters					Freundlich parameters		
	$Q_m$ mg/g	$K_L$ L/g	$R_L$	$\Delta G^\circ$ kJ/mol	$r^2$	$K_F$	$1/n$	$r^2$
CX700-30	69	0.154	0.047	- 19.6	0.997	3.6	0.632	0.911
CX700-60	133	0.277	0.107	- 22.7	0.999	11.1	0.420	0.942
CX700-90	103	0.168	0.075	- 21.3	0.999	9.5	0.449	0.925

Table 7: Comparison of adsorption capacities of PNP onto various carbon adsorbents.

Adsorbents	Amount adsorbed (mg/g)	Refs
Activated carbons	116-212	[18]
Carbon fibers	155-258	[19]
Sawdust biochars	~ 29- 117	[33]
Microalgal biochar	~ 205	[34]
Nanographite oxide	~269	[35]
Oxidized graphite	333	[36]
Carbon xerogels	69-133	This work

In addition, Table 7 summarizes the adsorption capacity of PNP onto different carbon materials with our prepared carbon xerogels samples [18, 19, 33-36]. It can be disclosed that the capacity of PNP onto carbon xerogels prepared in this study is comparable or less than those reported by other carbon materials. Moreover, the adsorption rate using carbon xerogels is faster throughout their mesoporous structure as compared to these adsorbents in literature.

#### 4. Conclusions

The carbonization of resorcinol-formaldehyde templated on tannic acid for 60 min at 700°C yielded good mesoporous carbon material to be used as adsorbent. Results of liquid-phase

adsorption toward cadmium and p-nitrophenol confirmed the high performance of these materials. Maximum adsorption capacity of both cadmium ions and PNP onto the greatest carbon adsorbent (CX-700-60) sample was 99 and 133 mg/g, respectively.

Overall, the final characteristics of the prepared adsorbents; such as high total surface area, degree of mesoporosity as well as the active sites of surface functional groups are the most effective factors in the adsorption of cadmium and p-nitrophenol onto the prepared samples.

#### Conflict of interest

Authors declare that there is no conflict of interest

## References

- [1] M. Inagaki, F. Kang, Carbon materials science and engineering – From fundamentals to applications. Tsinghua University Press (2006).
- [2] J.M. D. Tascón, Novel Carbon Adsorbents, 1<sup>st</sup> edition, Copyright © Elsevier Ltd, 2012.
- [3] J. Goscianska, A. Olejnik, I. Nowak, M. Marciniak, R. Pietrzak, Stability analysis of functionalized mesoporous carbon materials in aqueous solution, Chem. Eng. J. 290 (2016) 209–219.
- [4] S.A.C. Carabineiro, M. F. R. Pereira, J. J.M. Órfão and J. L. Figueiredo, Surface chemistry of activated carbons, In: Activated carbon: Classifications, properties and preparation, J. F. Kwiatkowski (Ed.), Nova Science Publishers, Inc., chapter 1 (2011) 1-3.
- [5] E.I. Paez, M. Haro, Emilio J. Juarez-Pérez, R.J. Carmona, J. B. Parra, R. L. Ramos, C. O. Ania, Fast synthesis of micro/mesoporous xerogels: Textural and energetic Assessment, Microporous and Mesoporous Materials 209 (2015) 2–9.
- [6] N.A. Fathy, B.S. Girgis, L.B. Khalil, J.Y. Farah, Utilization of cotton stalks-biomass waste in the production of carbon adsorbents by KOH activation for removal of dye-contaminated water, Carbon Letters 11 (2010) 224-234.
- [7] B.S. Girgis, A.M. Soliman, N.A. Fathy, Development of micro mesoporous carbons from several seed hulls under varying conditions of activation, Micropor. Mesopor. Mater. 142 (2011) 518–525.
- [8] B. S. Girgis, I. Y. El-Sherif, A. A. Attia and N. A. Fathy, Textural and adsorption characteristics of carbon xerogel adsorbents for removal of Cu (II) ions from aqueous solution, J. Non-Crystalline Solids 358 (2012) 741-747.
- [9] J. Figueiredo, J. Sousa, C. Orge, M. Pereira and J. Órfão, Adsorption of dyes on carbon xerogels and templated carbons: influence of surface chemistry, Adsorption 17 (2011) 431–441.
- [10] S. Chandra, S. Bag, R. Bhar, P. Pramanik, Effect of transition and non-transition metals during the synthesis of carbon xerogels, Micropor. Mesopor. Mater. 138 (2011) 149–156.
- [11] B. Yang, C. Yu, Q. Yu, X. Zhang, Z. Li, L. Lei, N-doped carbon xerogels as adsorbents for the removal of heavy metal ions from aqueous solution, RSC Adv. 5 (2015) 7182-7191.
- [12] P. Veselá, V. Slovák, N-doped carbon xerogels prepared by ammonia assisted pyrolysis: Surface characterization, thermal properties and adsorption ability for heavy metal ions, J. Anal. Appl. Pyrol. 109 (2014) 266–271.
- [13] F. Yu, Y. Wu, J. Ma, C. Zhang, Adsorption of lead on multi-walled carbon nanotubes with different outer diameters and oxygen contents: Kinetics, isotherms and thermodynamics, J. Environ. Sci. 25 (2013) 195–203.
- [14] M.Y. Abdelnaeim, I.Y. El Sherif, A.A. Attia, N.A. Fathy, M.F. El Shahat, Impact of chemical activation on the adsorption performance of common reed towards Cu(II) and Cd (II), Intern. J. Mineral Proc. 157 (2016) 80–88.
- [15] M. Kobya, E. Demirbas, E. Senturk, M. Ince, Adsorption of heavy metal ions from aqueous solutions by activated carbon prepared from apricot stone. Bioresource Technol. 96 (2005) 1518–1521.
- [16] K. Yang, B. S. Xing, Adsorption of organic compounds by carbon nanomaterials in aqueous phase: Polanyi theory and its application, Chem. Rev. 110 (2010) 5989–6008.
- [17] L. A. Rodrigues, T. M. B. Campos, M. O. Alvarez-Mendes, A. D. R. Coutinho, K. K. Sakane and G. P. Thim, Phenol removal from aqueous solution by carbon xerogel, J. Sol–Gel Sci. Technol., 2012, 63(2), 202–210.
- [18] N.A. Fathy, S.A.S. Ahmed, R.M. M. Aboelenin, Effect of activation temperature on textural and adsorptive properties for activated carbon derived from local reed biomass: Removal of p-nitrophenol, Environ. Res. Eng. Management 1 (2012) 10-22.
- [19] S. El-Shafey, N.A. Fathy, L. Khalil, Abatement of p-nitrophenol from aqueous solutions using oxidized carbon fiber, Egypt. J. Chem. 60 (2017) 995- 1006.
- [20] S. Lagergren, Zur theorie der sogenannten adsorption gelöster stoffe. 591. Kungliga Svenska Vetenskapsakademiens, Handlingar 24, 1–39 (1898).
- [21] Y.S. Ho, G. McKay, Sorption of dye from aqueous solution by peat, Chem. Eng. J. 70, 115-124 (1998).
- [22] W.J. Weber, J.C. Morris, Kinetics of adsorption on carbon from solution, J. Sanit. Eng. Div. Am. Soc. Civ. Eng. 89, 31-60 (1963).
- [23] I. Langmuir, The adsorption of gases on plane surfaces of glass, mica and platinum, J. Am. Chem. Soc. 40, 1361-1403 (1918).
- [24] H.M.F. Freundlich, Over the adsorption in solution, J. Phys. Chem. 57, 385-470 (1906).
- [25] J. Balach, L. Tamborini, K. Sapag, D. F. Acevedo, C.A. Barbero, Facile preparation of hierarchical porous carbons with tailored pore size obtained using a cationic polyelectrolyte as a soft template, Coll. Surf. A: Physicochem. Eng. Aspects 415 (2012) 343– 348.
- [26] Badie S. Girgis, Amina A. Attia, Nady A. Fathy, Potential of nano-carbon xerogels in the

- remediation of dye-contaminated water discharges, *Desalination* 265 (2011) 169-176.
- [27] G. Amaral-Labat, A. Szczurek, V. Fierro, N. Stein, C. Boulanger, A. Pizzi, A. Celzard, Pore structure and electrochemical performances of tannin based carbon cryogels, *Biomass Bioenergy* 39 (2012) 274-82.
- [28] F. Braghiroli, V. Fierro, M.T. Izquierdo, J. Parmentier, A. Pizzi, A. Celzard, Nitrogen-doped carbon materials produced from hydrothermally treated tannin, *Carbon* 50 (2012) 5411-5420.
- [29] I.Y. El-Sherif, N.A. Fathy, Equilibrium and kinetic study of Cd (II) and Ni (II) ions removal by semi-carbonized/H<sub>3</sub>PO<sub>4</sub> cotton stalks, *Electronic J. Environ. Agricult. Food Chem.* 10 (2011) 2744-2758.
- [30] R. Leyva-Ramos, L.A. Bernal-Jacome, I. Acosta-Rodriguez, Adsorption of cadmium(II) from aqueous solution on natural and oxidized corncob, *Sep. Purif. Technol.* 45 (2005) 41-49.
- [31] C. Tang, Y. Shu, R. Zhang, X. Li, J. Song, Bing Li, Yuting Zhang, Danling Ou, Comparison of the removal and adsorption mechanisms of cadmium and lead from aqueous solution by activated carbons prepared from *Typha angustifolia* and *Salix matsudana*, *RSC Adv.*, 2017, 7, 16092-16103.
- [32] N.V. Perez-Aguilar, E. Munoz-Sandoval, P.E. Diaz-Flores, J.R. Rangel-Mendez, Adsorption of cadmium and lead onto oxidized nitrogen-doped multiwall carbon nanotubes in aqueous solution: equilibrium and kinetics, *J Nanopart Res* 12 (2010) 467-480.
- [33] L. Liu, G. Deng, X. Shi, Adsorption characteristics and mechanism of p-nitrophenol by pine sawdust biochar samples produced at different pyrolysis temperatures, *Scientific Reports* 10:5149 (2020) 1 -11.
- [34] H. Zheng, W. Guo, S. Li, Y. Chen, Q. Wu, X. Feng, R. Yin, S.-H. Ho, N. Ren, J.-S. Chang, Adsorption of p-nitrophenols (PNP) on microalgal biochar: Analysis of high adsorption capacity and mechanism, *Bioresour. Technol.* 244 (2017) 1456-1464.
- [35] B. Zhang, F. Li, T. Wu, D. Sun, Y. Li, Adsorption of p-nitrophenol from aqueous solutions using nanographite oxide, *Colloids and Surfaces A: Physicochem. Eng. Aspects* 464 (2015) 78-88.
- [36] N.A. Fathy, R.R. Abd El-Latif, R.M. M. Aboelenin, L.B. Khalil, Green reduction of oxidized graphite to reduced graphene oxide using *Zygophyllum album* L.f.: Comparative adsorption studies on p-nitrophenol, *Recent Innov. Chem. Eng.* 8 (2015) 87-102.